JOURNAL OF CATALYSIS 99, 19–27 (1986)

Effect of Thermal Treatments on the Properties of V_2O_5/TiO_2 and MoO_3/TiO_2 Systems

MARGARITA DEL ARCO, M. JESÚS HOLGADO, CRISTINA MARTÍN, AND VICENTE RIVES

Departamento de Química Inorgánica, Facultad de Farmacia, Universidad de Salamanca, Apdo. 449, 37071 Salamanca, Spain

Received August 12, 1985; revised November 12, 1985

The surface properties of TiO_2 (anatase)-supported V_2O_5 and MoO_3 have been studied, as well as the effect of calcination at 773 K on the porosity of the samples, before and after incorporation of the supported phase. While for the support and for the MoO_3/TiO_2 samples a steady decrease in the surface area is observed with the thermal treatments and molybdena seems to have no effect on the pore structure of the carrier, incorporation of V_2O_5 has a dramatic effect on it, destroying the pore structure and sharply decreasing the surface area, irrespective of any thermal treatment on the support. No rutilization is observed in any case. The results are interpreted by assuming the formation of patches of vanadium pentoxide on the surface of the support, and the formation of continuous films of MoO_3 on the carrier. © 1986 Academic Press, Inc.

INTRODUCTION

Vanadium oxide-based catalysts are widely used for selective oxidation of hydrocarbons. However, to achieve good activity and selectivity levels, V_2O_5 should be dispersed on a support. From the recent review by Wainwright and Foster (*1*) it is concluded that, by far, the most successful support is titania, normally used in the form of anatase. The TiO_2–V_2O_5 is a classical example of support-enhancement of the active phase, specially if the metal oxide is applied to the carrier surface as a monomolecular layer. Titania-supported molybdenum oxide has also been widely studied for this same type of reaction, in an attempt to correlate the surface structure and the catalytic activity (*2–7*).

From these studies, it may be concluded that: (i) the starting metal salt may influence the state of the final catalyst; (ii) the interaction of the starting metal salt and the titania support takes place through the surface hydroxyl groups of the latter; (iii) for low Mo and V contents the corresponding oxides are dispersed on the support, and maximum catalytic activity is achieved when a monolayer of MoO_3 (or V_2O_5) is formed around the TiO_2 particles, but for large contents, bulk MoO_3 or V_2O_5 are formed (*8*); (iv) even with a V_2O_5 loading equivalent to three monolayers, the TiO_2 surface is not completely covered by V_2O_5, but exposed to the reactants (*9*).

However, the effect of the supported phase on the pore structure of the catalyst, and the effect of thermal treatments given to the support before the incorporation of the supported phase have been very scarcely investigated, despite their expected influence on the final catalysts and therefore on their catalytic activity. Very recent results with the V_2O_5/TiO_2 system indicate that the anatase-containing catalysts show higher activity and selectivity in *o*-xylene oxidation, while the properties of systems obtained using rutile resemble those of pure vanadia (*10*). As mentioned above, when V_2O_5 is incorporated onto TiO_2, two types of vanadia are present: surface vanadia species, responsible for the oxidation of *o*-xylene, and V_2O_5 crystallites (whose percentage increases with the V_2O_5 content) that seem to be inactive in the catalytic reaction (*11, 12*).

The effect of thermal treatments given to the support before the incorporation of the

0021-9517/86 $3.00

supported phase is studied in the present paper and V_2O_5/TiO_2 and MoO_3/TiO_2 catalysts have been prepared. As described below, the amounts of supported phases were chosen to be equivalent to two monolayers, and, in the case of the vanadium catalyst, it corresponds to the composition range where the larger activity for ethanal formation from ethanol has been observed (*13*).

EXPERIMENTAL

Materials

The support (T1) was TiO_2 kindly given by Dr. T. A. Egerton, from Tioxide International, U.K. (Ref. CLD1161/C). It had been obtained by precipitation from titanyl sulfate and calcined at 673 K for 19 h; XRF analysis indicated the presence of SO_3 (7.01%) and P_2O_5 (0.01%) as the main impurities. According to its X-ray diffraction profile, it is pure anatase, but badly crystallized, with a specific surface area (BET) of 114.9 $m^2\ g^{-1}$, that decreased to 59.1 $m^2\ g^{-1}$ after heating in 40 kN m^{-2} O_2 at 773 K for 5 h, thus leading to support T2 (*14*).

Loading of V_2O_5 or MoO_3 was performed by a conventional impregnation technique, dissolving 1.306 g NH_4VO_3 (Panreac, prs) or 1.352 g $(NH_4)_6Mo_7O_{24} \cdot 4H_2O$ (Carlo Erba, rpe) in 50 ml bidistilled water (containing a small amount of oxalic acid in the case of the metavanadate solution to improve its solubility), the solution being slowly added, while stirring, to 3 g of TiO_2. The pHs of the solutions were 2.5 and 4.5 for the metavanadate and molybdate salts, respectively; under these conditions, the predominating species is VO_2^+ for vanadium (*15*) while for molybdenum an equilibrium exists between MoO_4^{2-} and $Mo_7O_{24}^{6-}$ (*16*). ESCA and ISS data by Houalla *et al.* (*17*) for MoO_3/Al_2O_3 systems show that at pH ca. 4 an improvement of Mo dispersion is achieved. The amounts of vanadium and molybdenum salts were chosen taking into account the surface covered by a $VO_{2.5}$ (10.3×10^4 pm^2) or a MoO_3 (15×10^4 pm^2) "molecule" (*18, 19*), and the surface of the original T1 support (114.9 $m^2\ g^{-1}$), to yield final materials where the amounts of V_2O_5 or MoO_3 equal two monolayers of the supported phase. After impregnation, the suspension was stirred at room temperature overnight and the solvent slowly evaporated at 340–350 K. The solid thus obtained was calcined in 40 kN m^{-2} O_2 at 773 K for 5 h and manually grounded in an agate mortar, leading to samples VT1 (vanadia–titania) and MT1 (molybdena–titania). Similar materials, VT2 and MT2, were obtained upon impregnation of the support T2, i.e., support T1 heated in oxygen *before* incorporation of vanadium or molybdenum oxides. The composition of the samples correspond to $TiV_{0.3}O_{2.75}$ and $TiMo_{0.2}O_{2.6}$ (34 and 36% V_2O_5 and MoO_3 (w/w), respectively).

Apparatus

The X-ray diffraction profiles were recorded in a Philips PW 1030 instrument, using Ni-filtered Cu$K\alpha$ radiation (λ = 154.05 pm) and standard conditions.

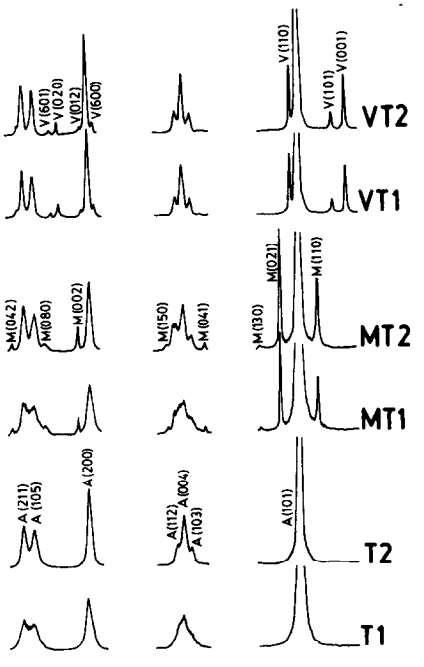

FIG. 1. Selected portions of the X-ray diffraction diagrams of the supports (T1, T2) and the samples (VT1, VT2, MT1, MT2). Peaks of anatase (A), molybdena (M), and vanadia (V) are indicated.

Magnetic measurements were carried out at room temperature in a Stanton MC-5 Gouy balance equipped with a Newport C electromagnet and using $Hg[Co(SCN)_4]$ as reference for calibrating the tube.

The electronic spectra of the samples in the range 880–230 nm were obtained in a Shimadzu UV-240 spectrophotometer provided with a diffuse reflectance accessory and a Shimadzu PR-1 graphic printer, and using MgO or untreated parent TiO_2 as the reference, with a slit of 5 nm.

The nitrogen (from S.C.O., 99.995%) adsorption isotherms (77 K) were measured in a conventional Pyrex high-vacuum system (residual pressure less than 10^{-4} N m^{-2}), equipped with a mercury vapor diffusion pump, Macleod gauge, and grease-free stopcocks. Pressure changes were monitored with a MKS pressure transducer. The system was calibrated previously with helium (S.C.O., 99.998%).

RESULTS AND DISCUSSION

X-Ray Diffraction

Selected portions of the X-ray diffraction profiles of both supports and all four samples have been included in Fig. 1. In all six cases, the peak at 352 pm ($2\theta = 25.28°$) corresponding to diffraction by planes (101) of anatase, was the most intense, while the most intense peak of rutile at 325 pm ($2\theta = 27.4°$), planes (110), was detected for no sample. This indicates that the thermal treatment of the pure support, or after incorporation of the vanadium or molybdenum oxides, does not change the crystallographic phase of TiO_2.

For samples containing vanadium, in addition to the peaks due to diffraction by anatase, some other peaks were detected. All these additional peaks correspond to the presence of V_2O_5, and ascription of the peaks has been done in Fig. 1 by comparison with literature data (*20*) for orthorhombic V_2O_5 (synthetic shcherbinaite). The presence of no other oxide of vanadium, nor ternary V–Ti–O compounds, was observed.

Finally, in samples containing molybdenum, the peaks detected correspond only to orthorhombic molybdite, MoO_3 (*21*), together with those of anatase and no peak to ternary Mo–Ti–O compounds nor lower Mo oxide was observed.

Besides these identification data, some other interesting features can be observed in this figure. Although the original support shows the peaks of anatase, these are very broad and the triplet at ca. 240 pm ($2\theta = 37.4°$) due to diffraction by planes (103), (004), and (112), as well as the doublet at ca. 170 pm ($2\theta = 53.9°$) due to diffraction by planes (105) and (211), are not very well defined indicating a lack of good crystallinity. When the support is calcined at 773 K, the X-ray diffraction pattern of support T2 shows an improvement in the sharpness of these peaks, indicating a crystallization and/or an increase in the crystallite size as a consequence of heating. It should be noted that samples T2, VT1, and MT1 were given *one* thermal treatment at 773 K, while samples VT2 and MT2 had been given *one* treatment before the incorporation of V or Mo, and a *second* heating after that. However, sample VT1 shows very well defined, sharp peaks, even better than those of support T2, and the triplet at 240 pm and the doublet at 170 pm are very well resolved. The situation does not change for sample VT2 (that had been given *two* heating treatments). The behavior of the molybdenum-containing samples is, however, different: for sample MT1 the shape and sharpness of the anatase peaks are quite similar to those of support T1, despite the fact that sample MT1 had been heated in O_2 at 773 K and support T1 had not, and for samples MT2, heated twice, the anatase peaks are rather similar to those for support T2, heated only once at 773 K. It seems that the presence of molybdenum delays the crystallization or the sintering of the support, while the presence of vanadium favors it. If the degree of crystallinity is tentatively measured from

the sharpness of the peaks, it increases in the order T1 ≲ MT1 < T2 ≲ MT2 ≪ VT1 = VT2.

Magnetic Measurements

Although the X-ray diffraction data above indicate the presence of TiO_2, V_2O_5, and MoO_3 as the only compounds existing in the samples, the possible presence of genotypic molybdenum oxides (*22*) makes worthwhile investigating the presence of molybdenum ions in an oxidation state lower than six.

To determine the susceptibilities of the samples, as the expected content in paramagnetic species was very low, the diamagnetic corrections were carried out from the experimental diamagnetism of the unloaded support T1. The measured susceptibilities (in the range 2 to 6 × 10^{-6} g^{-1}) increased with decreasing field strength, indicating the presence of a slight paramagnetism, probably due to the presence of impurities (10 ppm of the Fe according to the supplier); plots of susceptibility against reciprocal field were linear and were extrapolated to infinite field to eliminate the effect of ferromagnetism (*23*). The average susceptibility for samples containing Mo was -0.6×10^{-6} g^{-1}, and 0.2×10^{-6} g^{-1} for those having V. These results indicate that the samples are essentially diamagnetic, and thus the presence of lower oxides of Mo or V can be discarded.

Electronic Spectra

These have been collected in Fig. 2, together with the spectra of some reference compounds (TiO_2, MoO_3, V_2O_5). Reference V_2O_5 was obtained by calcination of $(NH_4)VO_3$ at 773 K, and reference MoO_3 was obtained by calcination of $(NH_4)_6Mo_7O_{24} \cdot 4H_2O$ at 773 K. While both supports are white, MoO_3 is slightly yellow and V_2O_5 is brick-red, samples MT1 and MT2 are pale blue, and samples VT1 and VT2 are slightly greenish yellow.

The spectra of samples VT1, VT2, support T1, and of a mechanical mixture V_2O_5/TiO_2 (containing the same relative amounts of V_2O_5 and TiO_2 that samples VT) are shown in Fig. 2A, where they have been vertically displaced for clarity.

The spectrum of the support, recorded against MgO (Fig. 2Aa), shows a very intense band rising below ca. 380 nm that has been ascribed (*24*) to an $O^{2-} \rightarrow Ti^{4+}$ charge transfer process. As this band is recorded for all samples, support T1 was used as ref-

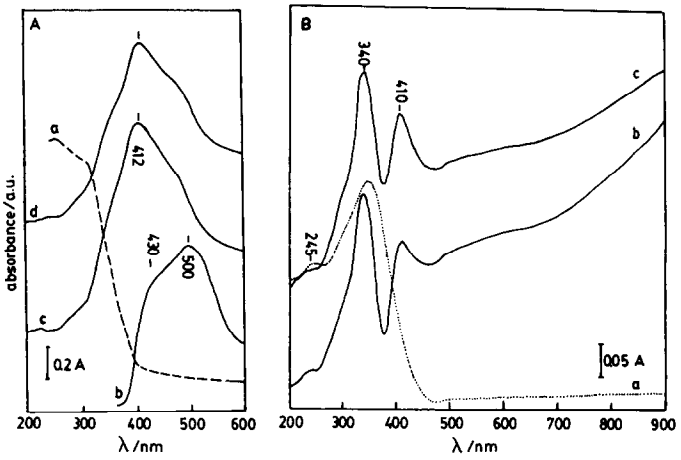

FIG. 2. Electronic spectra (diffuse reflectance) of the samples and of model compounds. (A) V-Containing solids: (a) parent TiO_2, (b) mechanical mixture V_2O_5/TiO_2, (c) sample VT1, (d) sample VT2. (B) Mo-Containing solids: (a) mechanical mixture MoO_3/TiO_2, (b) sample MT1, (c) sample MT2.

erence to record the spectra of other samples containing V or Mo.

Spectrum in Fig. 2Ab, corresponding to the mechanical mixture V_2O_5/TiO_2, shows two charge transfer maxima at 430 and 500 nm, responsible for the color of the vanadium pentoxide.

The spectra of samples VT1 and VT2 (Figs. 2Ac and d) show a very intense band at 412 nm, with a prominent shoulder at ca. 500 nm that correspond to the charge transfer maxima in Fig. 2Ab. However, the relative intensities of the bands at 412–430 and 500 nm have changed from the mechanical mixture V_2O_5/TiO_2 to the VT1 and VT2 samples, where the very intense band at 412 nm dominates the spectra.

A similar behavior is observed for the molybdenum-containing samples. While the corresponding MoO_3/TiO_2 mechanical mixture shows (Fig. 2Ba) an intense band at 740 nm with a prominent shoulder at 245 nm indicating the presence of octahedral [MoO_6] units (*25*), the spectra of samples MT1 and MT2 show, in addition, an absorption band at 410 nm together with a general absorbance increase all along the visible region (Figs. 2Bb and c). This absorption above 500 nm is responsible for the pale blue color shown by these samples. Although at first instance it may be ascribed to the presence of Mo^{5+} (d^1) species, for which two bands due to crystal field transitions in the range 1000–500 nm are expected (*26*), the magnetic results above indicate that such species do not exist in our samples. Moreover, they are hardly to be expected after the oxidizing way the samples have been obtained. It may be pointed out that Weyl and Förland have mentioned (*27*) a blue–grey color, not removed by oxidation, when high-valency ions are introduced interstitially into a titania powder, and a partial migration of Mo^{6+} ions into the subsurface layers of the lattice may have taken place, bearing in mind the closeness of Ti^{4+} and Mo^{6+} radii (74.5 and 73 pm, respectively, in octahedral coordination) (*28*).

A band at 415–410 nm has been previously observed by several authors when recording the visible spectra of titanium dioxide and titanates doped with several first transition series cations such as Cr, Mn, Co, Ni, Cu (*24, 29–33*), and it has been ascribed to a $M^{n+} \rightarrow Ti^{4+}$ charge transfer process, i.e., the excitation of an electron from the M^{n+} cation into the conduction band of the semiconducting support. However, in our case, vanadium and molybdenum exist in oxidation states +5 and +6, respectively (d^0 configuration in both cases), according to the X-ray diffraction data and magnetic measurements above, and then such an interpretation is not valid in this case, as our guest cations have no *d* electron to be promoted to the conduction band of TiO_2. The origin of this band needs to be further confirmed, although preliminary studies in this laboratory suggest that it is due to the formation of oxygen-containing species (*34*) on the surface of the titania, in some way stabilized by the presence of the guest cations.

Nitrogen Adsorption Isotherms

The curves for all six samples have been plotted in Fig. 3. The analysis of such isotherms for pore size distribution have been carried out following the method by Cranston and Inkley (*35*) and the de Boer's *t*-plot method (*36*) has been applied as well. The numerical calculations have been performed with the assistance of a BASIC program developed by us (*14*), run in an Olivetti L1-M 20 personal computer (PCOS operative system) coupled to an Olivetti PR-1450 graphic printer.

The isotherms for supports T1 and T2 show two different types of hysteresis loops, corresponding to types H2 and H1, respectively, in Sing's classification (*37*), and due to bottleneck type and cylindrical pores open at both ends, respectively. A mere opening of the "cul-de-sac" pores by the thermal treatment should be ruled out, as this process would imply an increase in the specific surface area and, on the other

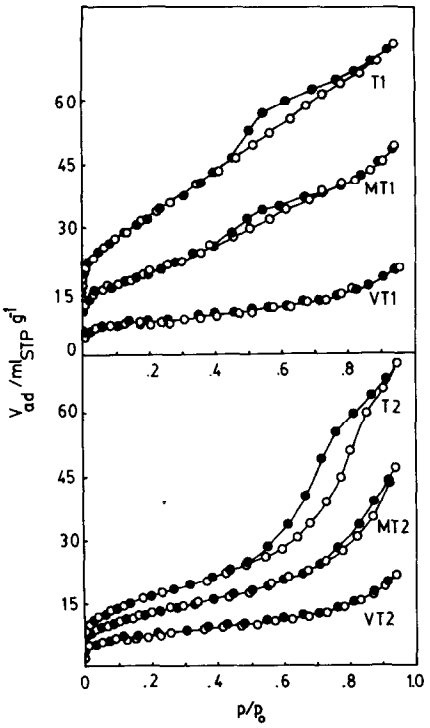

FIG. 3. Nitrogen adsorption isotherms (77 K) for the supports and the samples.

hand, according to the pore size distributions in Fig. 4, the pores existing in support T2 are wider than those in support T1. The average particle sizes for these two supports, from the breadth of the main X-ray diffraction peak of anatase at 352 pm (*14*), are 15 and 23 nm for supports T1 and T2, respectively; i.e., the sizes of the pores are ca. 25% of the average particle sizes of the solids. So, it can be assumed that the mesopores existing in these two supports are simply interparticle channels that in support T1 can be partially obstructed by other (smaller) crystallites, thus leading to the "cul-de-sac" pores, while in support T2 the partial sintering of the smaller particles by the thermal treatment has opened these pores; the specific surface areas for these supports roughly coincide with the geometrical values obtained from the crystallite sizes and the specific gravity of the anatase.

The persistence of these same hysteresis loops in samples MT1 and MT2 indicate that such shaped pores exist also in these samples, and the incorporation of molybdenum in sample MT1 has avoided the changes observed in sample T2, obtained by heating support T1. On the contrary, curves for samples VT1 and VT2 were identical, without any hysteresis loop, and coincident for both samples. The presence of vanadium thus leads to deep changes in the structure of the solid, whichever the pore structure (bottleneck pores, T1, or cylindrical pores, T2) of the starting support.

Cumulative surface areas and pore size distribution curves have been included in Fig. 4, while numerical data are summarized in Table 1. Curves in Fig. 4 show that heating of the support leads to development of mesopores in the range 5–7 nm diameter, decreasing the contribution by pores with a diameter close to 2 nm. These changes can also be concluded from the changes in the shape of the S_C curves for both supports. In samples containing molybdenum, however, the main contributions to surface area come from pores with $d \lesssim 6$ nm (MT1) or $d \lesssim 4$ nm (MT2), while both V-containing samples show contributions only by pores with $d > 2$ nm. First we will discuss the changes observed in the supports, and then we will turn to the Mo- and V-containing samples.

As shown in Table 1, the cumulative surface values for samples T1, T2, MT1, and MT2 (i.e., those showing hysteresis loops) are *always* larger than the corresponding

TABLE 1

BET-, Cumulative-, and *t*-Surface Area Values for the Supports and the Samples[a]

		T1	T2	MT1	MT2	VT1	VT2
S_{BET}		114.9	59.1	66.8	44.3	24.5	24.6
S_C		134.7	83.7	78.6	53.2	24.2	23.5
S_t[b]	S_{t1}	—	58.1	59.0	45.1	25.0	24.8
	S_{t3}	18.9	22.4	22.0	—	—	—

[a] Units in $m^2\ g^{-1}$.

[b] S_{t1} and S_{t3} correspond to the values determined from the first and the third linear segments in the V-*t* plot, respectively, as counted from the left-hand side.

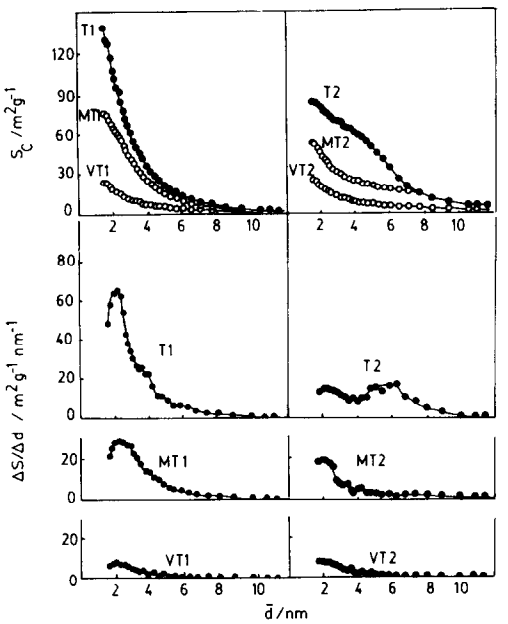

FIG. 4. Cumulative surface plots and pore size distribution curves for the supports and the samples.

BET values, the differences being well above the experimental error; on the contrary, both sets of values coincide in the case of samples VT1 and VT2, where reversible isotherms are obtained. With regards to the V-*t* plots of de Boer, sigmoid curves with up to three linear segments were obtained in some cases, and micropores were absent in all six samples. For these sigmoid V-*t* plots the surface area can be estimated from the slope of the first linear segment, S_{t1} (as counted from the left-hand side of the plot), while the determination of the external surface area is carried out from the slope of the third linear segment, S_{t3} (*38*). For support T2, S_{t1} equals 58.1 m^2 g^{-1} (in good agreement with the BET value) and S_{t3} 22.4 m^2 g^{-1}, its sum amounting to 80.5 m^2 g^{-2}, roughly matching the cumulative surface area calculated for this sample. For support T1, however, the first linear segment is not observed, and so S_{t1} could not be determined; nevertheless, the difference between S_C and S_{t3} (18.9 m^2 g^{-1} for S_{t3}) equals 115.8 m^2 g^{-1}, coincident with the BET value of 114.9 m^2 g^{-1}.

It can then be concluded that when shaped pores exist, leading to isotherms with hysteresis loops (at least those corresponding to types H2 and H1) capillary condensation leads to S_C values larger than those obtained by the BET method (these BET values coinciding with the S_{t1} ones), by a value corresponding to the external surface still available for adsorption after capillary filling (S_{t3}).

The same effect is observed for samples MT1 and MT2, although in this case the matching between S_{BET} and S_{t1} (66.8 and 59.0 m^2 g^{-1} for sample MT1, and 44.3 and 45.1 m^2 g^{-1} for sample MT2) and between S_C and $S_{t1} + S_{t3}$ is only roughly coincident for sample MT1.

On the contrary, in the case of the vanadium-containing samples, the values obtained by the BET and cumulative methods coincide very well, and match those obtained from the essentially linear V-*t* plots for these samples, within experimental error; i.e., the incorporation of vanadium has completely destroyed the pore system existing in the support, promoting its sintering.

FINAL REMARKS

From the results above, it can be concluded that molybdenum and vanadium behave differently when incorporated on the surface of titanium dioxide (anatase). In the case of molybdenum the incorporation takes place with the formation of bulk MoO_3, but sintering of the support crystallites does not take place further than that observed for a pure support similarly heated, and the pore structure of the carrier is respected. The same effect is observed if the pores existing in the support are modified by a thermal treatment previous to the incorporation of the molybdenum. On the contrary, although V_2O_5 crystallites grow in the case of the VT1 and VT2 samples, the sintering causes a sharp decrease in the surface area, destroying the pore structure of the support, irrespective of any thermal

treatment given to the carrier before the incorporation of the supported phase.

An interpretation at the atomic level for this difference is lacking in the literature, but should be obviously related to the structure and chemistry of the supported phases finally formed. Both oxides show layered structures, the main differences corresponding to the (slightly) more regular structure for MoO_3 than for V_2O_5. From EXAFS studies, Pettifer *et al.* have shown (*39*) that an epitactic model between anatase and V_2O_5 is not applicable in these catalysts.

With respect to MoO_3, Courtine *et al.* (*40*) have claimed that the (100) and (010) planes of MoO_3 can be "anchored" on the (010) and (001) planes of anatase, thus suggesting an easiness for growing of MoO_3 layers on these faces of the TiO_2 crystallites.

So, a tentative explanation for the different behavior observed for V_2O_5/TiO_2 and MoO_3/TiO_2 may be given if it is assumed that, both supported phases interacting through the hydroxyl groups, the growth of the V_2O_5 crystallites does not take place uniformly, giving rise to islands of V_2O_5, leaving part of the support surface covered, and this growth may bring together and sinter different TiO_2 particles. On the contrary, if MoO_3 grows epitactically on the TiO_2 crystallites, the interparticle pores will not be destroyed, leaving the particles apart and thus a sharp decrease in the surface area as an effect of sintering will not be observed.

An alternative explanation, assuming that the V_2O_5 (or MoO_3) crystallites grow only by their own, without any interaction with the support particles, should be ruled out, as, in such a case, the behavior of both sets of samples would be the same; in the case of the Mo-containing samples, MT1 had been given one thermal treatment at 773 K, as support T2, but although both show similar surface area values, the adsorptive behavior is different: heating of the pure support leads to a change in the pore shapes and thus the hysteresis loops in the nitrogen adsorption isotherms are different for supports T1 and T2; however, the hysteresis loops for samples T1 and MT1 are similar (bottleneck pores), indicating that the changes performed by the pure support T1 when heated (supported T2) have not taken place place when T1 is heated after incorporation of molybdenum. For the V-containing samples, the effect on the surface area and on the shape of the nitrogen adsorption isotherm are sufficiently evident to discard this independent-growing model.

ACKNOWLEDGMENTS

Authors' thanks are due to Dr. T. A. Egerton (Tioxide International, U.K.) for gift of the samples, and to Professor M. Sánchez Camazano (Centro de Edafología y Biología Aplicada, CSIC, Salamanca, Spain) for her assistance in obtaining the X-ray diffraction data. Partial support by CAICYT (Grant 282-84) is greatly acknowledged.

Note added in proof. After this work was completed, Ng and Gulari (*J. Catal.* **92,** 340, 1985) and Lin *et al.* (*J. Catal.* **94,** 108, 1985) have shown that tetrahedral molybdate species exist on TiO_2 at submonolayer coverages, while any amount in excess of a monolayer is converted to bulk-like MoO_3.

REFERENCES

1. Wainwright, M. S., and Foster, N. R., *Catal. Rev.* **19,** 211 (1979).
2. Adzhamov, K. Yu., Senchikhina, A. K., Alkazov, T. G., and Mekhtiev, K. M. *Kinet. Catal.* **16,** 589 (1975).
3. Akimoto, M., and Echigoya, E., *J. Catal.* **29,** 191 (1973).
4. Rivasseau, J., Canesson, P., and Blanchard, M., *J. Phys. Chem.* **84,** 2972 (1980).
5. Tanaka, K., Miyahara, K., and Tanaka, K., *Bull. Chem. Soc. Japan* **54,** 3106 (1981).
6. Ai, M., *Bull. Chem. Soc. Japan* **49,** 1328 (1976).
7. Ono, T., Nakagawa, Y., Miyata, H., and Kubokawa, Y., *Bull. Chem. Soc. Japan* **57,** 1205 (1984).
8. Bond, G. C., and Brückman, K., "Selectivity in Heterogeneous Catalysis" (Faraday Discussion No. 72), p. 235. Royal Society of Chemistry, London, 1981.
9. Inomata, M., Mori, K., Miyamoto, A., Ui, T., and Murakami, Y., *J. Phys. Chem.* **87,** 754 (1983).
10. Gasior, M., Gasior, I., and Grzybowska, B., *Appl. Catal.* **10,** 87 (1984).

11. van Hengstum, A. J., Ommen, J. G., Bosch, H., and Gellings, P. J., *Appl. Catal.* **8,** 369 (1984).

12. Nachs, I. E., Saleh, R. Y., Chan, S. S., and Chersich, C. C., *Appl. Catal.* **15,** 339 (1985).

13. Nakagawa, Y., Ono, T., Miyata, H., and Kubokawa, Y. *J. Chem. Soc., Faraday Trans. 1* **79,** 2929 (1983).

14. Martin, C., Rives, V., and Malet, P., *Powder Technol.,* in press.

15. Clark, R. J. H., *in* "Comprehensive Inorganic Chemistry" (J. C. Bailar, Jr., H. J. Emeleus, R. Nyholm, and A. F. Trotman-Dickenson, Eds.), Vol. 3, p. 520. Pergamon, Oxford, 1973.

16. Rollinson, C. L., *in* "Comprehensive Inorganic Chemistry" (J. C. Bailar, Jr., H. J., Emeleus, R. Nyholm, and A. F. Trotman-Dickenson, Eds.), Vol. 3, p. 379. Pergamon, Oxford, 1973.

17. Houalla, M., Kibby, C. L., Petrakis, L., and Hercules, D. M., *J. Catal.* **83,** 50 (1983).

18. Roozeboom, F., Fransen, T., Mars, P., and Gellings, P. J., *Z. Anorg. Allg. Chem.* **449,** 25 (1979).

19. Fransen, T., van Berge, P. C., and Mars, P., *in* "Preparation of Catalysts" (B. Delmon, P. A. Jacobs, and G. Poncelet, Eds.), p. 405. Elsevier, Amsterdam, 1976.

20. Joint Committee on Powder Diffraction Standards, File No. 9-387 (1971).

21. Joint Committee on Powder Diffraction Standards, File No. 5-0508 (1971).

22. Cotton, F. A., and Wilkinson, G., "Advanced Inorganic Chemistry," 1980, 4th Ed., Chap. 22, p. 848. Wiley, New York, 1980.

23. Selwood, P., "Magnetochemistry," 2nd Ed., p. 45. Interscience, London, 1956.

24. Borgarello, E., Kiwi, J., Grätzel, M. Pelizzetti, E., and Visca, M., *J. Amer. Chem. Soc.* **104,** 2996 (1982).

25. Massoth, F.E., *in* "Advances in Catalysis" (D. D. Eley, H. Pines, and P. B. Weisz, Eds.), Vol. 27, p. 265. Academic Press, New York, 1978.

26. Level, A. B. P., "Inorganic Electronic Spectroscopy," 2nd ed., p. 393. Elsevier, Amsterdam, 1984.

27. Weyl, W. A., and Förland, T., *Ind. Eng. Chem.* **42,** 257 (1950).

28. Huheey, J. E., "Inorganic Chemistry: Principles of Structure and Reactivity," 3rd ed., Chap. 3, p. 73. Harper & Row, Cambridge, 1983.

29. Mackor, A., and Blasse, G., *Chem. Phys. Lett.* **77,** 6 (1981).

30. de Korte, P. H. M., 't Lam, R. U. E., Schoonman, J., and Blasse, G., *J. Inorg. Nucl. Chem.* **43,** 2261 (1981).

31. Blasse, G., de Korte, P. H. M., and Mackor, A., *J. Inorg. Nucl. Chem.* **43,** 1499 (1981).

32. Criado, J. J., Macias, B., Martín, C., and Rives, V., *J. Mater. Sci.* **20,** 1427 (1985).

33. Criado, J. J., Macias, B., and Rives, V., *React. Kinet. Catal. Lett.* **27,** 313 (1985).

34. Che, M., and Tench, A. J., *in* "Advances in Catalysis" (D. D. Eley, H. Pines, and P. B. Weisz, Eds.), Vol. 32, p. 1. Academic Press, New York, 1983.

35. Cranston, R. W., and Inkley, F. A., *in* "Advances in Catalysis" (D. D. Eley, H. Pines, and P. B. Weisz, Eds.), Vol. 9, p. 143. Academic Press, New York, 1957.

36. Lippens, B. C., and de Boer, J. H., *J. Catal.* **4,** 319 (1965).

37. Sing, K. S. W., Everett, D. H., Haul, R. A. W., Moscou, L., Pierotti, R. A., Rouquerol, J., and Siemieniewska, T., *Pure Appl. Chem.* **57,** 603 (1985).

38. Jaycock, M. J., and Parffit, G. D., "Chemistry of Interfaces," p. 226. Wiley, New York, 1981.

39. Kozlousky, R., Pettifer, R. F., and Thomas, J. M., *J. Phys. Chem.* **87,** 5172 (1983).

40. Bordes, E., Jung, S. J., and Courtine, P., *in* "Proceedings, 9th Iberoamerican Symposium on Catalysis" (M. Farinha Portela, Ed.), p. 983. Lisboa, 1984.